

CANADIAN APPLIED  
MATHEMATICS QUARTERLY  
Volume 10, Number 2, Summer 2002

## LEAST-SQUARES SEISMIC MIGRATION USING WAVEFIELD PROPAGATORS FOR AVP INVERSION

*Based on a presentation at the PIMS-MITACS Workshop on  
Inverse Problems and Imaging, University of British Columbia,  
June 9–10, 2001.*

HENNING KUEHL AND MAURICIO D. SACCHI

**ABSTRACT.** The imaging of geological subsurface structures with seismic reflection energy is a powerful tool for the detection and the assessment of hydrocarbon reservoirs. The seismic method can be understood as a multi-source and multi-receiver reflection scattering experiment. The seismic sources and receivers are placed at the earth's surface. The sources emit seismic energy into the subsurface and the receivers record the earth's response (the backscattered energy) as a function of time and position relative to the source. The goal of seismic imaging is to invert the recorded seismograms for the subsurface structures and their underlying lithological properties. Seismic imaging is usually called migration when only structural image information is desired. The term inversion is used if the goal is to invert for physical properties of the subsurface. In this paper, we do not attempt to invert for true physical parameters. Instead, we aim at preserving the angle or the closely related ray-parameter dependence of migrated seismic data. In a subsequent step, this information can then be used to invert for the lithological parameters that determine the angle/ray-parameter dependent subsurface reflectivity. In the framework of linearized scattering theory seismic data modelling and migration is defined as a pair of adjoint operators. This definition leads to the formulation of an iterative least-squares seismic migration method. The modelling/migration operator pair is implemented using a wavefield propagator technique. We propose least-squares migration with a regularization term that imposes continuity on amplitude variations as a function of ray-parameter (AVP). This regularization is based on the idea

---

AMS subject classification: 86A15.

Copyright ©Applied Mathematics Institute, University of Alberta.

that roughness along the ray-parameter axis stems from numerical artifacts and incompletely and/or irregularly sampled seismic wavefields. A synthetic seismic data example is given for illustration.

**1 Introduction.** Most common seismic imaging techniques can be subdivided into two categories. The first category are algorithms that back-propagate the seismic surface wavefield into the earth using recursive propagators. These algorithms are frequently called wave-equation migration/inversion techniques. The second category are algorithms based on ray-tracing. They are often referred to as Kirchhoff-type imaging techniques. In ray-tracing, problems with shadow zones and caustics can occur depending on the complexity of the geology of the subsurface. Furthermore, the ability of the ray-based approach to account for multi-pathing is limited. Propagator techniques, on the other hand, allow the seismic waves to travel along all possible ray-paths (Gray and May, [11]).

The formulation of migration/inversion algorithms starts with the definition of a subsurface model in terms of physical parameters and a reflection scattering mechanism. To make the imaging problem tractable we make simplifying assumptions about the model and its interactions with the seismic wavefield. Based on the work of Clayton and Stolt [6], we then derive a forward modelling formula that relates the adopted subsurface model with the seismic data. The ultimate goal in migration/inversion is to solve the forward relationship for the unknown subsurface model parameters. However, we must keep in mind that, in practice, our simplified model serves merely as a proxy for the more general nature of the problem. We must therefore interpret the results with care.

In order to invert the generally “ill-posed” problem we employ a least-squares data fitting method. This allows us to regularize the least-squares solution by imposing certain desirable characteristics and constraints.

Nemeth et al. [20] and Duquet et al. [8] followed the least-squares approach to obtain Kirchhoff-type least-squares imaging techniques. In this paper we investigate the possibility of using wavefield propagators instead.

In the first part of this paper, we briefly review seismic data modelling based on linear scattering theory. Furthermore, we discuss the use of Green’s functions for seismic modelling in spatially varying reference media. This leads to a linear operator equation that relates the subsur-

face reflectivity with the seismic data. This review is mostly based on a paper by Stolt and Weglein [26].

Next, we introduce a phase-shift propagator method to compute Green's functions in laterally invariant media that is described in Clayton and Stolt [6].

The computation of the least-squares inverse requires the knowledge of the adjoint of the modelling operator. The adjoint operator can be regarded as a first approximation to the inverse problem (Claerbout, [5]). In fact, applying the adjoint operator is often sufficient for structural imaging. In this paper we define migration as the adjoint of modelling. Following Stolt and Weglein [26] we describe how to extract amplitude variation with angle (AVA) information from the migrated wavefield.

Since propagator techniques are most beneficial when applied to imaging problems in complex environments, the modelling/migration operators are generalized for laterally varying media. This can be achieved by expanding the operators used by Clayton and Stolt [6]. The expansion we adopt here results in extended split-step propagators for modelling and migration (Gazdag and Sguazzero, [10]; Stoffa et al., [25]; Kessinger, [13]; Margrave and Ferguson, [18]).

As an alternative to AVA imaging/inversion one can use the offset ray-parameter to obtain amplitude variation with ray-parameter (AVP) information (de Bruin et al., [7]; Prucha et al., [23]; Mosher and Foster, [19]). In this paper we will choose the AVP over the AVA parameterization.

To complete the discussion on migration using AVP imaging we briefly mention the possibility to improve the adjoint operator by considering the so-called imaging Jacobian (Stolt and Benson, [27]; Sava et al., [24]). The analytical imaging Jacobian can also be used to precondition the iterative least-squares migration discussed in the last part.

In least-squares migration we use the above generalized modelling/migration operators to formulate a least-squares migration/inversion scheme. We introduce a regularization of the inverse problem that appears particularly beneficial when the emphasis is on obtaining amplitude variation with ray-parameter (AVP) information. An example based on the synthetic Marmousi data set (Versteeg and Grau, [28]) is given for illustration.

**2 Seismic data modelling under the Born approximation.**  
Consider the 3-D acoustic wave-equation with variable density  $\rho(\mathbf{x})$  and

compressional velocity  $\alpha(\mathbf{x})$  in the frequency domain:

$$(1) \quad \begin{aligned} \mathcal{D}(\mathbf{x}, \omega)\Psi(\mathbf{x}, \mathbf{s}, \omega) &= \left( \nabla \cdot \frac{1}{\rho(\mathbf{x})}\nabla + \frac{\omega^2}{\rho(\mathbf{x})\alpha^2(\mathbf{x})} \right) \Psi(\mathbf{x}, \mathbf{s}, \omega) \\ &= -\delta(\mathbf{x} - \mathbf{s}), \end{aligned}$$

where the time-dependence of the wavefield  $\Psi(\mathbf{x}, \mathbf{s}, \omega)$  is given by  $e^{-i\omega t}$ . The operator  $\mathcal{D}(\mathbf{x}, \omega)$  is the variable density Helmholtz operator. The vector  $\mathbf{x} = (x, y, z)$  denotes the spatial position in a coordinate system with the positive  $z$  component pointing down into the earth (Figure 1). The vector  $\mathbf{s}$  is the position of the point source and the compressional velocity  $\alpha(\mathbf{x})$  and density  $\rho(\mathbf{x})$  are spatially varying. We define the bulk-modulus  $K(\mathbf{x}) = \rho(\mathbf{x})\alpha^2(\mathbf{x})$  and follow Stolt and Weglein [26] and cast the problem as a perturbation about a reference solution by introducing the reference operator  $\mathcal{D}_0$ :

$$(2) \quad \mathcal{D}_0(\mathbf{x}, \omega) = \nabla \cdot \frac{1}{\rho_0(\mathbf{x})}\nabla + \frac{\omega^2}{K_0(\mathbf{x})},$$

where  $K_0(\mathbf{x})$  and  $\rho_0(\mathbf{x})$  are slowly varying local averages of the true values  $K(\mathbf{x})$  and  $\rho(\mathbf{x})$ , too slowly varying to produce significant reflection energy.

The scattering operator (scattering potential)  $\mathcal{V}(\mathbf{x}, \omega)$  that generates the seismic reflection data is defined as:

$$(3) \quad \begin{aligned} \mathcal{V}(\mathbf{x}, \omega) &= \mathcal{D}(\mathbf{x}, \omega) - \mathcal{D}_0(\mathbf{x}, \omega) \\ &= \nabla \cdot \left( \frac{1}{\rho(\mathbf{x})} - \frac{1}{\rho_0(\mathbf{x})} \right) \nabla + \omega^2 \left( \frac{1}{K(\mathbf{x})} - \frac{1}{K_0(\mathbf{x})} \right) \\ &= \nabla \cdot \left( \frac{a_2(\mathbf{x})}{\rho_0(\mathbf{x})} \right) \nabla + \omega^2 \left( \frac{a_1(\mathbf{x})}{K_0(\mathbf{x})} \right), \end{aligned}$$

where  $a_1(\mathbf{x}) = \frac{\rho_0(\mathbf{x})}{\rho(\mathbf{x})} - 1 = \frac{\Delta\rho(\mathbf{x})}{\rho(\mathbf{x})}$  and  $a_2(\mathbf{x}) = \frac{K_0(\mathbf{x})}{K(\mathbf{x})} - 1 = \frac{\Delta K(\mathbf{x})}{K(\mathbf{x})}$ . The coefficients  $a_1(\mathbf{x})$  and  $a_2(\mathbf{x})$  are unknown fractional changes of the medium properties describing the subsurface. The differential operators in the term containing  $a_2$  cause an angle dependence of the scattering potential.

We substitute  $\mathcal{D} = \mathcal{V} + \mathcal{D}_0$  in equation (1) and obtain:

$$(4) \quad \mathcal{D}_0\Psi(\mathbf{x}, \mathbf{s}) = -\mathcal{V}\Psi(\mathbf{x}, \mathbf{s}) - \delta(\mathbf{x} - \mathbf{s}).$$

## LEAST-SQUARES SEISMIC MIGRATION

311

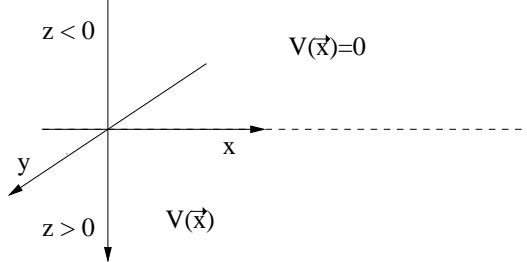


FIGURE 1: The coordinate system with the  $z$  axis pointing into the earth. The scattering potential  $\mathcal{V}$  is zero for  $z < 0$ . The integration boundaries in equation (5) span the entire (model) space. A free surface boundary is not considered.

The solution of (4) can be written as an integral equation (Lippman–Schwinger equation):

$$(5) \quad \Psi(\mathbf{x}, \mathbf{s}, \omega) = \Psi_0(\mathbf{x}, \mathbf{s}, \omega) + \int d\mathbf{x}' \Psi_0(\mathbf{x}, \mathbf{x}', \omega) \mathcal{V}(\mathbf{x}', \omega) \Psi(\mathbf{x}', \mathbf{s}, \omega),$$

where

$$(6) \quad \mathcal{D}_0 \Psi_0(\mathbf{x}, \mathbf{s}) = -\delta(\mathbf{x} - \mathbf{s}).$$

The solution  $\Psi_0(\mathbf{x}, \mathbf{s})$  is the Green's function propagating through the known reference medium. The band-limited seismic scattering data are given by:

$$(7) \quad \Psi_s(\mathbf{r}, \mathbf{s}, \omega) = S(\omega)[\Psi(\mathbf{x}, \mathbf{s}, \omega) - \Psi_0(\mathbf{x}, \mathbf{s}, \omega)],$$

where  $S(\omega)$  represents the band-limited source signature. Using the first order Born approximation (single scattering approximation) we substitute  $\Psi(\mathbf{x}, \mathbf{s}, \omega) = \Psi_0(\mathbf{x}, \mathbf{s}, \omega)$  in (5) and obtain a linearized modelling equation for the seismic data:

$$(8) \quad \Psi_s(\mathbf{r}, \mathbf{s}, \omega) = S(\omega) \int d\mathbf{x} \Psi_0(\mathbf{r}, \mathbf{x}, \omega) \mathcal{V}(\mathbf{x}, \omega) \Psi_0(\mathbf{x}, \mathbf{s}, \omega),$$

where the vector  $\mathbf{r}$  denotes the seismic receiver position. We note that the single scattering assumption can be a significant source of error. We

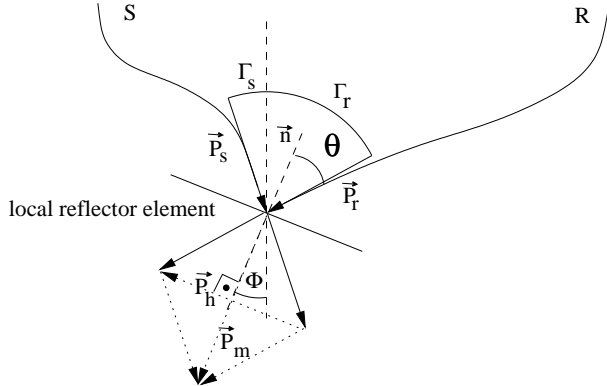


FIGURE 2: A source/receiver ray-pair that is coincident at a subsurface position. The source and receiver slowness vectors  $\mathbf{p}_s$  and  $\mathbf{p}_r$  are tangential to the rays. At the point of coincidence they describe a rhombus with diagonals  $\mathbf{p}_m$  and  $\mathbf{p}_h$ . The diagonals are perpendicular with respect to each other. If we assume a (locally) plane reflector the angle of incidence is given by  $\theta = \arctan(\frac{|\mathbf{p}_h|}{|\mathbf{p}_m|})$ . The vector  $\mathbf{p}_h$  is parallel to the reflector plane and the vector  $\mathbf{p}_m$  is parallel to the reflector normal  $\mathbf{n}$ .

interpret the scattering potential  $\mathcal{V}(\mathbf{x}, \omega)$  by way of ray-theory. Invoking the high-frequency approximation for the Green's functions of the reference operator  $\mathcal{D}_0$  yields for the source (Beydon and Keho, [2]):

$$(9) \quad \Psi_0(\mathbf{x}, \mathbf{s}, \omega) = A(\mathbf{x}, \mathbf{s}) e^{i\omega\tau(\mathbf{x}, \mathbf{s})}.$$

The term  $A(\mathbf{x}, \mathbf{s})$  is the slowly varying amplitude determined by the transport equation (Bleistein, [3]):

$$(10) \quad 2\nabla\tau \cdot \nabla \left( A \frac{1}{\sqrt{\rho_0}} \right) + \Delta\tau \left( A \frac{1}{\sqrt{\rho_0}} \right) = 0,$$

and  $\tau$  is the traveltime given by the eikonal equation:

$$(11) \quad (\nabla\tau)^2 = \frac{1}{\alpha_0^2(\mathbf{x})} = \mathbf{p}_s \cdot \mathbf{p}_s.$$

The vector  $\nabla\tau = \mathbf{p}_s$  is the slowness vector and is everywhere tangential to the ray-path. The slowness vector has magnitude  $\alpha_0^{-1}(\mathbf{x})$  (slowness).

The functions  $\tau$  and  $A$  must also satisfy  $\tau = 0$  for  $\mathbf{x} = \mathbf{s}$  and  $|\mathbf{x} - \mathbf{s}|A \rightarrow 1/4\pi$ , as  $\mathbf{x} \rightarrow \mathbf{s}$  (Bleistein, [3]).

Using the high frequency approximation in equation (8) and integration by parts yields:

$$(12) \quad \Psi_s(\mathbf{r}, \mathbf{s}, \omega) = \omega^2 S(\omega) \int d\mathbf{x} A(\mathbf{r}, \mathbf{x}) A(\mathbf{x}, \mathbf{s}) \frac{v(\mathbf{x}, \theta)}{K_0(\mathbf{x})} e^{iw(\tau(\mathbf{x}, \mathbf{r}) + \tau(\mathbf{x}, \mathbf{s}))},$$

where:

$$(13) \quad v(\mathbf{x}, \theta) = a_1(\mathbf{x}) + \cos(2\theta)a_2(\mathbf{x}).$$

The angle  $2\theta$  is the angle between the local source slowness vector  $\mathbf{p}_s$  and the local receiver slowness vector  $\mathbf{p}_r$  at the depth-point where the two ray-paths coincide (Figure 2). The source and receiver slowness vectors describe a rhombus with diagonals  $\mathbf{p}_m = \mathbf{p}_r + \mathbf{p}_s$  and  $\mathbf{p}_h = \mathbf{p}_r - \mathbf{p}_s$ . If we interpret the reflection scattering to be caused by a (locally) plane reflector (specular reflection), the diagonals are directly related to reflector dip  $\Phi$  and angle of incidence  $\theta$  as demonstrated in Figure 2. As we shall see later, the vectors  $\mathbf{p}_m$  and  $\mathbf{p}_h$  are also related to the midpoint-offset domain, a coordinate system frequently used in seismic processing.

For simplicity we restrict the theory to the two-dimensional case. If we assume a line source and invariant medium properties along the  $y$  direction, equation (12) simplifies to:<sup>1</sup>

$$(14) \quad \begin{aligned} \Psi_s(r, 0|s, 0, \omega) &= \omega^2 S(\omega) \iint dx dz A(r, 0|x, z) A(x, z|s, 0) \\ &\times \frac{v(x, z, \theta)}{K_0(x, z)} e^{iw(\tau(x, z|r, 0) + \tau(x, z|s, 0))}, \end{aligned}$$

where we have switched from the vector to a coordinate notation. Furthermore, we assume that sources and receivers are placed along a level datum at  $z = 0$ . Equation (14) can be implemented by calculating the amplitude terms and traveltimes numerically using a (paraxial) ray-tracing algorithm (Beydon and Keho, [2]). However, here we would like to employ a wavefield propagator technique. We abandon the ray-theoretical Green's functions and write equation (14) again in the more

---

<sup>1</sup>Strictly speaking, this formula is only valid when applied to synthetic data based on the two dimensional wave-equation. When dealing with real-world data 2½-D effects should be considered (Stolt and Weglein, [26]; Bleistein, [3]).

general form:

$$(15) \quad \begin{aligned} & \Psi_s(r, 0|s, 0, \omega) \\ &= \omega^2 S(\omega) \iint dx dz \Psi_0(r, 0|x, z, \omega) \frac{v(x, z, \theta)}{K_0(x, z)} \Psi_0(x, z|s, 0, \omega). \end{aligned}$$

The interpretation of the interaction between the reflector element and the wavefield remains valid since it involves only local quantities at the reflection point.

**2.1 Modelling using propagators in laterally invariant reference media.** For *laterally invariant reference media* the Green's functions in equation (15) can be replaced by the WKBJ Green's function obtained for the depth-separated wave equation (Clayton and Stolt, [6]). The depth separation is achieved by Fourier transforms along the horizontal coordinates in equation (6). The Green's function for the source has the analytical expression (Clayton and Stolt, [6]):

$$(16) \quad \Psi_0(x, z|s, 0, \omega) = \frac{\sqrt{\rho_0(z)\rho_0(0)}}{2\pi} \int dk_{sx} e^{ik_{sx}(s-x)} \frac{ie^{i\omega \int_0^z p_{sz}(z') dz'}}{2\omega \sqrt{p_{sz}(z)p_{sz}(0)}},$$

where  $p_{sz}$  is the vertical receiver slowness component. The vertical slowness component is calculated from the horizontal source wavenumber  $k_{sx}$  and the dispersion relation of the wave equation:

$$(17) \quad \omega p_{sz}(z) = k_{sz}(z) = \frac{\omega}{\alpha_0(z)} \sqrt{1 - \frac{k_{sx}^2 \alpha_0^2(z)}{\omega^2}},$$

where  $k_{sz}(z)$  is the vertical source wavenumber. The receiver Green's function is obtained in an analogous way. Inserting the Green's functions in (15) gives the modelling formula in the frequency-wavenumber (Clayton and Stolt, [6]; Stolt and Benson, [27]):<sup>2</sup>

$$(18) \quad \begin{aligned} \Psi_s(k_{rx}, 0|k_{sx}, 0, \omega) &= -\omega^2 S(\omega) \int dz \frac{\rho_0(0)\rho_0(z)}{4\sqrt{k_{rz}(0)k_{rz}(z)k_{sz}(0)k_{sz}(z)}} \\ &\times \frac{v(k_{rx} + k_{sx}, z, \theta)}{K_0(k_{rx} + k_{sx}, z, \theta)} e^{i \int_0^z k_{rz}(z') + k_{sz}(z') dz'}. \end{aligned}$$

---

<sup>2</sup>Rather than defining new symbols when a function is transformed to a new domain, we use the same symbol with the new arguments.

$$\begin{array}{ll}
 \mathbf{k}_s = (k_{sx}, k_{sz}) & \mathbf{k}_r = (k_{rx}, k_{rz}) \\
 \mathbf{p}_s = \frac{\mathbf{k}_s}{\omega} & \mathbf{p}_r = \frac{\mathbf{k}_r}{\omega} \\
 \mathbf{p}_s = \frac{(\sin \Gamma_s, \cos \Gamma_s)}{\alpha_0} & \mathbf{p}_r = \frac{(\sin \Gamma_r, \cos \Gamma_r)}{\alpha_0} \\
 \mathbf{k}_m = \mathbf{k}_s + \mathbf{k}_r & \mathbf{k}_h = \mathbf{k}_r - \mathbf{k}_s \\
 \mathbf{p}_m = \frac{\mathbf{k}_m}{\omega} & \mathbf{p}_h = \frac{\mathbf{k}_h}{\omega} \\
 \mathbf{k}_s = 1/2(\mathbf{k}_m - \mathbf{k}_h) & \mathbf{k}_r = 1/2(\mathbf{k}_m + \mathbf{k}_h) \\
 k_{sz} = \frac{\omega}{\alpha_0} \sqrt{1 - \frac{\alpha_0^2 k_{sx}^2}{\omega^2}} & k_{rz} = \frac{\omega}{\alpha_0} \sqrt{1 - \frac{\alpha_0^2 k_{rx}^2}{\omega^2}}
 \end{array}$$

TABLE 1: Important relationships in source-receiver and midpoint-offset coordinates.

The sum of the source and receiver surface wavenumbers in the scattering potential suggests that there exists a more convenient coordinate system. We transform equation (18) to midpoint offset coordinates<sup>3</sup> by defining midpoint and offset wavenumbers<sup>4</sup>  $\mathbf{k}_m = (k_{mx}, k_z) = \mathbf{k}_s + \mathbf{k}_r$  and  $\mathbf{k}_h = (k_{hx}, k_{hz}) = \mathbf{k}_r - \mathbf{k}_s$ , respectively. The modelling formula (18) reads now:

(19)

$$\begin{aligned}
 \Psi_s(k_{mx}, 0 | k_{hx}, 0, \omega) = & -\omega^2 S(\omega) \int dz \frac{\rho_0(0)\rho_0(z)}{4\sqrt{k_{rz}(0)k_{rz}(z)k_{sz}(0)k_{sz}(z)}} \\
 & \times \frac{v(k_{mx}, z, \theta)}{K_0(k_{mx}, z, \theta)} e^{i \int_0^z k_z(z') dz'}.
 \end{aligned}$$

The vertical source and receiver wavenumbers are calculated from their midpoint-offset counterparts (Table 1) by the relationships  $\mathbf{k}_s = 1/2(\mathbf{k}_m - \mathbf{k}_h)$  and  $\mathbf{k}_r = 1/2(\mathbf{k}_m + \mathbf{k}_h)$ . It is important to note that we restrict equation (19) to real values of  $k_z$ . That is, evanescent energy is not considered in the following.

The angle  $\theta$  in the scattering potential is an implicit function of the midpoint and offset wavenumbers. To see this, we note that we have  $\mathbf{p}_m \cdot \mathbf{p}_h = 0$  at the point where source and receiver rays are coincident.

<sup>3</sup>The horizontal midpoint-offset space coordinates are given by the transformation  $m = \frac{r+s}{2}$  and  $h = \frac{r-s}{2}$  at the source-receiver datum.

<sup>4</sup>To avoid more notational clutter we use  $k_z$  rather than  $k_{mz}$  for the vertical midpoint wavenumber.

From Figure 2 we find (Stolt and Weglein, [26]):

$$(20) \quad \tan \theta = \frac{|\mathbf{p}_h|}{|\mathbf{p}_m|} = \frac{p_{hx}}{p_{mz}} = \frac{k_{hx}}{k_z}.$$

The ray-parameters in (20) are understood to be taken at the reflection point.

The horizontal slowness components are constant along the rays, since there are no lateral velocity variations in the reference medium. This fact can be used to formulate modelling/migration algorithms that operate directly in the horizontal offset ray-parameter domain (Ottolini, [21]). However, we will drop this assumption further below which will make the recalculation of the horizontal wavefield spectrum at each depth level inevitable.

To simplify the notation the data modelling formula (19) is written in terms of a symbolic operator notation. First we define an angle-dependent model function  $f$  by:

$$(21) \quad f\left(k_{mx}, \frac{k_{hx}}{k_z}, z\right) = \frac{-\omega^2 v(k_{mx}, z, \arctan(\frac{k_{hx}}{k_z}))}{K_0(k_{mx}, z, \arctan(\frac{k_{hx}}{k_z}))}.$$

This function is made suitable for wavefield propagation by mapping  $f(k_{mx}, \frac{k_{hx}}{k_z}, z)$  to  $f(k_{mx}, k_{hx}, z)$  in a preparation step prior to modelling:

$$(22) \quad f(k_{mx}, k_{hx}, z) = \mathcal{F}_z^{-1} \mathcal{R}'_\theta \mathcal{F}_z f\left(k_{mx}, \frac{k_{hx}}{k_z}, z\right),$$

where  $\mathcal{F}_z$  and  $\mathcal{F}_z^{-1}$  are the forward and inverse Fourier transform along  $z$ , respectively. The operator  $\mathcal{R}'_\theta$  is the adjoint of the radial-trace transform  $\mathcal{R}_\theta$  from the  $(k_z, k_{hx})$  to  $(k_z, \theta)$  space.<sup>5</sup> This mapping procedure is illustrated in Figure 3.

The forward modelling operation is now written symbolically as:

$$(23) \quad \Psi(k_{mx}, 0 | k_{hx}, 0, \omega) = \int dz \mathcal{A} \mathcal{P} f(k_{mx}, k_{hx}, z),$$

with the diagonal WKBJ amplitude scaling operator:

$$(24) \quad \mathcal{A} = \frac{\rho_0(0)\rho_0(z)}{4\sqrt{k_{rz}(0)k_{rz}(z)k_{sz}(0)k_{sz}(z)}}$$

<sup>5</sup>The radial-trace transform  $\mathcal{R}_\theta$  is equivalent to the more intuitive slant-stack (Ottolini, 1984) in the offset-depth domain.

## LEAST-SQUARES SEISMIC MIGRATION

317

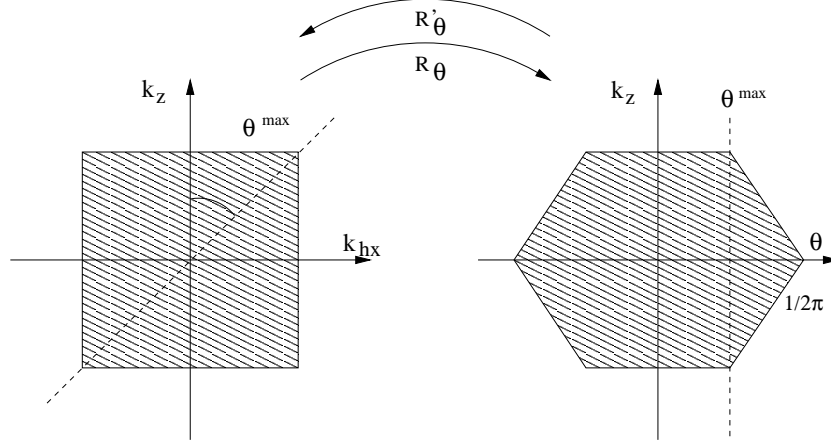


FIGURE 3: The radial trace transform  $\mathcal{R}_\theta$  extracts the wavefield along radial lines in the  $(k_z, k_{hx})$  space and maps the result into the  $(k_z, \theta)$  space. The limited range of the offset wavenumbers due to the finite acquisition aperture causes truncation effects in the  $(k_z, \theta)$  space. The adjoint operator  $\mathcal{R}'_\theta$  maps the angle-dependent model function  $f$  from the  $(k_z, \theta)$  space to the  $(k_z, k_{hx})$  space. In modelling,  $\mathcal{R}'_\theta$  is applied as a preparation step to make the model function suitable for the DSR phase-shift propagator. In migration,  $\mathcal{R}_\theta$  is used to convert the function  $f(k_{mx}, k_{hx}, k_z)$  into the angle dependent function  $f(k_{mx}, \frac{k_{hx}}{k_z}, k_z)$  (after Sava et al., [24]).

and the propagator:

$$(25) \quad \mathcal{P} = e^{i \int_0^z k_z(z') dz'}.$$

The operator  $\mathcal{P}$  is known as the DSR (double-square-root) phase-shift propagator (Gazdag, [9]). For a given model function  $f(k_{mx}, k_{hx}, z)$  the data  $\Psi(k_{mx}, 0|k_{hx}, 0, \omega)$  are obtained by propagating the model contributions for all  $z$  and summing them into the data-space function  $\Psi(k_{mx}, 0|k_{hx}, 0, \omega)$ . We have omitted  $S(\omega)$  for simplicity but keep in mind that all frequency dependent quantities are bandlimited. The complete modelling procedure is summarized with the application of

the operator  $\mathcal{L}$ :

$$\begin{aligned} \Psi(k_{mx}, 0 | k_{hx}, 0, \omega) &= \int dz \mathcal{P} \mathcal{F}_z^{-1} \mathcal{R}'_\theta \mathcal{F}_z f\left(k_{mx}, \frac{k_{hx}}{k_z}, z\right) \\ (26) \quad &= \mathcal{L} f\left(k_{mx}, \frac{k_{hx}}{k_z}, z\right). \end{aligned}$$

Notice that we have conveniently dropped the scaling factor  $\mathcal{A}$  in equation (26). In fact, Wapenaar [30] shows that this is justified, since the employed Green's function should be normalized with respect to the energy flux across interfaces separating regions of different medium parameters. Effectively, energy flux normalization amounts to a cancellation of the WKBJ amplitude term  $\mathcal{A}$  and warrants that seismic reciprocity is honored (Wapenaar, [30]).

**3 Seismic migration.** Our goal is to invert the seismic data for the angle dependence of  $f(k_{mx}, \frac{k_{hx}}{k_z}, z)$ . The function  $f$  is determined by the two unknowns  $a_1$  and  $a_2$ . Here, we are just concerned with producing an estimate of the amplitude variation with incident angle (AVA) of  $f(k_{mx}, \frac{k_{hx}}{k_z}, z)$ . In fact, the relevance of the quantities  $a_1$  and  $a_2$  for seismic inversion is debatable (Wapenaar, [29]). Seismic data are mostly generated by reflecting interfaces. For a plane wave incident on a plane reflecting interface in an elastic medium the Zoeppritz equations determine the amplitude behavior as a function of angle (Aki and Richards, 1980). Stolt and Weglein [26] relate the scattering potential to the linearized Zoeppritz equation (Aki and Richards, [1]) for the reflection of a compressional wave on a plane interface. However, to achieve this they introduce additional scaling factors and a normal derivative to be applied during inversion. Instead, Wapenaar [29] demonstrates that these steps are not necessary and that the scattering potential can be identified directly with the reflection coefficient for specularly reflected compressional waves. That is, the particular form of the scattering potential is merely an artifact of the linear Born approximation and, for specular reflections, can be replaced *ad hoc* by the specular reflectivity function (Bleistein et al., [4]). However, we must keep in mind that the assumption of a low contrast medium due to the linear Born approximation (weak scattering) is implicit in our formulas. This is because transmission loss due to energy partitioning at the interfaces and multiple scattering are not accounted for.

In any case, the function  $f(k_{mx}, \frac{k_{hx}}{k_z}, z)$  exhibits angle dependence and the migration/inversion should attempt to preserve this dependence as

faithfully as possible. Ideally, we would like to carry out the inversion for  $f(k_{mx}, \frac{k_{hx}}{k_z}, z)$  in the least-squares sense by minimizing an appropriate cost function. The first step to finding the least-squares solution is to formulate the adjoint operator  $\mathcal{L}'$  defined by  $\langle \Psi, \mathcal{L}f \rangle_\omega = \langle \mathcal{L}'\Psi, f \rangle_z$ , where the brackets represent the (complex) inner products in the data and model space, respectively. The adjoint operator can be seen as a first approximation to the inverse problem (Claerbout, [5]). In fact, we define seismic migration as the adjoint of the modelling operator (26). The application of the migration operator  $\mathcal{L}'$  gives the estimate:

$$(27) \quad \begin{aligned} \tilde{f}\left(k_{mx}, \frac{k_{hx}}{k_z}, z\right) &= \mathcal{F}_z^{-1} \mathcal{R}_\theta \mathcal{F}_z \int d\omega \mathcal{P}' \Psi(k_{mx}, 0 | k_{hx}, 0, \omega) \\ &= \mathcal{L}' \Psi(k_{mx}, 0 | k_{hx}, 0, \omega). \end{aligned}$$

The integral in equation (27) is the DSR migration formula. First, the data  $\Psi(k_{mx}, 0 | k_{hx}, 0, \omega)$  are downward propagated from the surface to the depth level  $z$  by the propagator  $\mathcal{P}'$ . Then they are summed over frequency to yield the model estimate  $\tilde{f}(k_{mx}, k_{hx}, z)$  in terms of horizontal midpoint and offset wavenumber and depth  $z$ . The summation over frequency is known as the seismic imaging condition. The frequency summation is equivalent to evaluating the wavefield at  $t = 0$ . In other words, migration is achieved by propagation of the source-receiver wavefield to a depth-level  $z$  (downward continuation) and the application of the causality principle. When the migration is complete for all  $z$ , the cascaded operators  $\mathcal{F}_z^{-1} \mathcal{R}_\theta \mathcal{F}_z$  are applied to  $\tilde{f}(k_{mx}, k_{hx}, z)$  as a post-processing step. The operator  $\mathcal{R}_\theta$  is the radial-trace transform shown in Figure 3. The angle transformed function  $\tilde{f}(k_{mx}, \frac{k_{hx}}{k_z}, z)$  exhibits an approximation of the amplitude variation with angle (AVA) information we are seeking. We remark that the AVA fidelity of migration can be improved by considering additional measures to obtain a better “approximate inverse” to the modelling relationship. We will discuss this point in the section on offset ray-parameter imaging.

**4 Modelling and migration using recursive propagators in laterally varying reference media.** The propagators  $\mathcal{P}$  and  $\mathcal{P}'$  in (23) and (27) were derived under the assumption of laterally constant reference velocities. This restriction can be partially lifted by employing a recursive propagator approach. To this end we first discuss the computer implementation of the modelling and migration operators in more detail.

In a numerical implementation the integrals in the phase-shift operators of (23) and (27) are replaced by summations and  $dz$  becomes a finite depth interval  $\Delta z$ . The velocities are assumed to be constant along the vertical range  $\Delta z$ . The phase-shift propagator can then be implemented as a non-recursive or recursive algorithm. In the non-recursive implementation the propagation between the surface-data and the depth-level  $z$  is carried out by computation of the complete phase-integral prior to propagation. In the recursive implementation the wavefield is successively propagated by iterative application of the phase-shift propagator in steps  $\Delta z$ .

Both implementations have certain advantages and disadvantages. Beneficial consequences of the non-recursive implementation are demonstrated in Kuehl and Sacchi [15]. However, in order to accommodate lateral velocity variations we must implement the modelling and migration formulas as recursive algorithms. This allows us to extend the phase-shift propagator by a local operator expansion. To this end we expand the square-root expression for the vertical source wavenumber in (17) using the split-step approximation (Stoffa et al., [25]). For the source we have:

$$(28) \quad k_{sz}(s, z) \approx \sqrt{\frac{\omega^2}{\alpha_0^2 \text{ref}(z)} - k_{sx}^2} + \left( \frac{\omega}{\alpha_0(s, z)} - \frac{\omega}{\alpha_0 \text{ref}(z)} \right).$$

The same approximation is used for the receiver square-root operator. The reference velocity  $\alpha_0 \text{ref}(z)$  is computed by laterally averaging the slowness variations for each propagation step  $\Delta z$ . The additional term in (28) is the split-step correction. It is applied at the source and receiver locations after the wavefield has been transformed to the space domain. This results in a recursive marching algorithm that alternates between the horizontal wavenumber and space domain at each depth level. This type of algorithm is known to give relatively accurate structural images even in complex media (Popovici, [22]).

The wide-angle accuracy of the split-step approximation can be improved by using multiple reference velocities for the propagation. The phase-shift propagators and the split-step correction are then applied in a data windowing mode (Gazdag and Sguazzero, [10]; Kessinger, [13]; Margrave and Ferguson, [18]). The standard and the windowed split-step approach can be applied to both the modelling and the migration operator.

### 5 Modelling and migration with the offset ray-parameter.

One may ask how meaningful the interpretation of  $\theta$  as the “angle of incidence” really is. In seismic imaging/inversion one deals mostly with regular geological interfaces. So one would like to relate the scattering potential to the reflectivity of the interfaces and interpret the angle  $\theta$  as the local angle of incidence. For this interpretation to be true, the interface curvature has to be moderate so that the reflection mechanism is predominantly specular. Furthermore, the conversion to “angle of incidence” is dependent on the reference velocity model (migration velocity field), since the vertical wavenumber is a function of  $\alpha_0$ . Unfortunately, the reference velocity is only known roughly in general. In practice, AVA estimation is an interpretive process and breaks down in areas where the above conditions are not fulfilled.

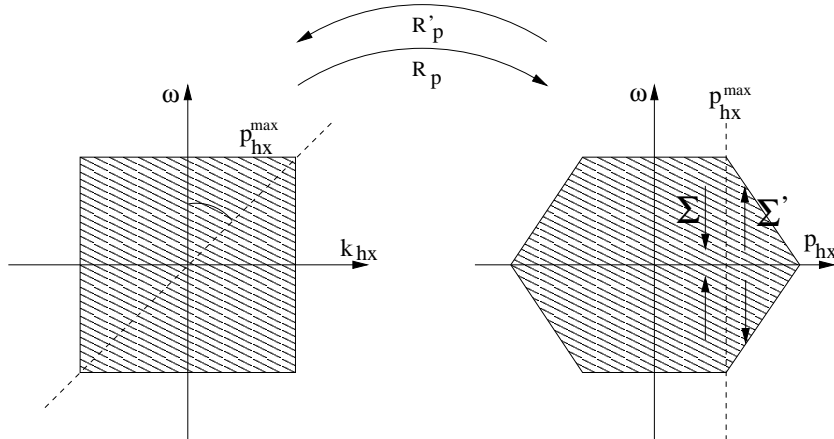


FIGURE 4: The radial trace transform  $\mathcal{R}_p$  extracts the wavefield along radial lines in the  $(\omega, k_{hx})$  space and maps the result into the  $(\omega, p_{hx})$  space. The limited range of the offset wavenumbers due to the finite acquisition aperture causes truncation effects in the  $(\omega, p_{hx})$  space. Since in offset ray-parameter imaging the radial trace transform and the actual seismic imaging condition (summation over  $\omega$ ) are one processing step the imaging condition is included in this schematic diagram as the operator  $\Sigma$ . The operator  $\Sigma'$  is the adjoint of the imaging condition.  $\Sigma'$  is used to generate the ray-parameter dependent function  $f(k_{mx}, p_{hx}, \omega, z)$ . The adjoint operator  $\mathcal{R}'_p$  maps the function  $f(k_{mx}, p_{hx}, \omega, z)$  to  $f(k_{mx}, k_{hx}, \omega, z)$ . The convergent and divergent arrows indicate summation (integration) and “spreading”, respectively.

The uncertainty with respect to reference velocity field motivates an alternative approach to angle imaging. Instead of “angle of incidence” we use the horizontal offset ray-parameter to obtain an amplitude variation with ray-parameter (AVP) estimate of the subsurface (de Bruin et al., [7]; Prucha and Biondi, [23]; Mosher and Foster, [19]). This is achieved by parameterizing the model function  $f$  with  $p_{hx} = \frac{k_{hx}}{\omega}$  and by using the relation  $\theta = \arcsin(\frac{\alpha_0 p_{hx}}{2 \cos \Phi})$  (see Figure 2):  $f(k_{mx}, \frac{k_{hx}}{\omega}, \Phi, z)$ . The dip angle  $\Phi$  of the reflector element is now an implicit parameter of the model function  $f$  and is omitted in the following for convenience. A conversion from AVP to AVA requires the dip angle  $\Phi$  as an input parameter that is provided by an interpreter. The dip is measured on the structural image. Hence, we do not rely on the reference velocity field for the local dip information. This extra step could, in some cases, help to improve the robustness of AVA estimation.

The offset ray-parameter is a quantity belonging to the data space and not the model space. This is because of the  $\omega$  dependence of  $p_{hx}$ . In order to perform modelling we first map  $f(k_{mx}, \frac{k_{hx}}{\omega}, z)$  to  $f(k_{mx}, k_{hx}, \omega, z)$ :

$$(29) \quad f(k_{mx}, k_{hx}, \omega, z) = \mathcal{R}'_p f\left(k_{mx}, \frac{k_{hx}}{\omega}, z\right).$$

This mapping results in the “spreading” of the values  $f(k_{mx}, \frac{k_{hx}}{\omega}, z)$  along the  $\omega$  axis (Figure 4). The subsequent transform  $\mathcal{R}'_p$  is the adjoint of the radial trace transformation from the  $(\omega, k_{hx})$  to the  $(\omega, p_{hx})$  space as shown in Figure 4.

The modelling is completed by applying the DSR propagator and summing the contribution of all depth levels into the data function:

$$(30) \quad \Psi(k_{mx}, 0 | k_{hx}, 0, \omega) = \int dz \mathcal{P} f(k_{mx}, k_{hx}, \omega, z).$$

We note that the conversion from the model to the data space was achieved implicitly in equation (29). As opposed to the previously outlined AVA mapping, the ray-parameter conversion is absorbed in the modelling process. We write (29) and (30) in one symbolic operator equation:

$$(31) \quad \Psi(k_{mx}, 0 | k_{hx}, 0, \omega) = \int dz \mathcal{P} \mathcal{R}'_p f\left(k_{mx}, \frac{k_{hx}}{\omega}, z\right) = \mathcal{L} f\left(k_{mx}, \frac{k_{hx}}{\omega}, z\right).$$

The migration formula is again found by formulating the adjoint opera-

tor:

$$(32) \quad \tilde{f}\left(k_{mx}, \frac{k_{hx}}{\omega}, z\right) = \int dw \mathcal{R}_p \mathcal{P}' \Psi(k_{mx}, 0 | k_{hx}, 0, \omega) \\ = \mathcal{L}' \Psi(k_{mx}, 0 | k_{hx}, 0, \omega).$$

Again we can choose a recursive implementation of (31) and (32) and employ the (generalized) split-step operator expansion to make formulas suitable for laterally varying media.

The modelling/migration operator pair (31) and (32) is used in the next section to invert seismic data in the least-squares sense. If instead only the adjoint (migration) operator (32) is to be applied the approximation of the inverse problem can be improved as shown by Sava et al. [24]. Their technique involves the computation of the local imaging Jacobian  $J = \frac{d\omega}{dk_z}|_z$  (Stolt and Benson, [27]). For AVP imaging, the vertical wavenumber  $k_z$  must be expressed as a function of offset ray-parameter. The resulting diagonal operator  $J_p$  evaluated at depth  $z$  is used by Sava et al. [24] to obtain an analytical approximate inverse operator:

$$(33) \quad \tilde{f}_{\text{inv}}\left(k_{mx}, \frac{k_{hx}}{\omega}, z\right) = \int dw J_p^{-1} \mathcal{R}_p \mathcal{P}' \Psi(k_{mx}, 0 | k_{hx}, 0, \omega) \\ = \mathcal{L}'_{\text{inv}} \Psi(k_{mx}, 0 | k_{hx}, 0, \omega).$$

However, this approximation is not satisfactory if the inversion is plagued with, for instance, incomplete data sampling and numerical operator artifacts.

**6 Least-squares migration for AVP imaging.** In least-squares migration/inversion we use the modelling and migration operators to invert the linear system (Kuehl and Sacchi, [16]):

$$(34) \quad \Psi(m, 0 | h, 0, \omega) = \mathcal{L}f(m, p_{hx}, z) + n,$$

where  $\Psi(m, 0 | h, 0, \omega)$  is the often incomplete seismic data in the midpoint-offset space-domain and  $n$  represents the noise. The function  $f$  is the ray-parameter dependent model function in midpoint-depth coordinates. The operator  $\mathcal{L}$  now includes forward and backward Fourier transforms for midpoint and offset.

The following cost function is iteratively minimized by a gradient method (Hestenes and Stiefel, [12]):

$$(35) \quad F(f) = \|\mathcal{W}(\Psi(m, 0|h, 0, \omega) - \mathcal{L}f(m, p_{hx}, z))\|^2 + \lambda^2 \|\partial_{p_{hx}} f(m, p_{hx}, z)\|^2,$$

where  $\mathcal{W}$  is a diagonal weighting operator. The operator  $\mathcal{W}$  is derived from the data covariance matrix and has zero weights in the case of dead traces and non-zero weights for live traces (Kuehl and Sacchi, [14]). The minimization amounts to an iterative application of  $\mathcal{L}'$  and  $\mathcal{L}$ . Besides the data-misfit term, we have added a regularization term that penalizes “roughness” along the ray-parameter  $p_{hx}$ . The  $\lambda^2$  factor allows us to control the amount of smoothing. The concept of smoothing is based on the desire to retrieve a continuous function  $f$  along the ray-parameter axis. This is justified by the logic that the angle/ray-parameter dependence should be continuous. Discontinuities or rapid amplitude changes are attributed to missing data (data aliasing) and numerical operator artifacts.

**6.1 Synthetic data example.** We illustrate least-squares AVP imaging with ray-parameter smoothing using the Marmousi data set (Versteeg and Grau, [28]). The synthetic Marmousi data are based on a variable velocity (Figure 5) and density model (not shown). Since the data were modelled with the acoustic wave equation, the angle dependence of the reflectors corresponds to the AVA/AVP of a fluid-fluid interface.

Figure 6A is the AVP gather at midpoint 175 out of a total of 240 midpoint positions (see also Figure 5). To generate the gathers the migration operator in equation (33) was applied to the regularly sampled data set. The gathers were produced with offset ray-parameters ranging from 0 to 760  $\mu\text{s}/\text{m}$ . AVP effects and numerical imaging artifacts are apparent. We have previously shown for selected reflection events that the retrieved AVA/AVP matches the theoretical AVA/AVP closely (Kuehl and Sacchi, [17]).

To test the influence of missing data on the imaging result we randomly replaced 80% of the data with dead traces prior to migration. Figure 6B shows the resulting AVP gathers. They exhibit stronger incoherent noise and the continuity along the ray-parameter axis is deteriorated. The effect of least-squares migration with moderate ray-parameter smoothing is demonstrated in Figure 6C. This result was obtained after 3 iterations of the minimization algorithm (conjugate gra-

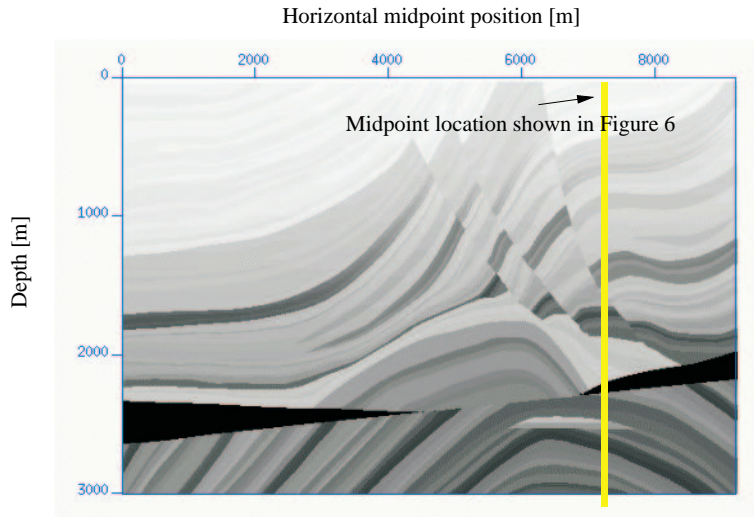


FIGURE 5: The Marmousi velocity model. The velocities range from 1500 to 5500 m/s. Darker shades denote higher velocities. The synthetic seismic data generated with a finite difference implementation of the acoustic wave-equation is widely used for benchmarking seismic imaging algorithms (Versteeg and Grau, [28]). The density model is not shown.

dients). Least-squares migration partially restores the continuity along the offset ray-parameter and improves the signal to noise ratio. After 6 iterations the smoothing effect is more pronounced and the amplitude variation is more smeared along the ray-parameter (Figure 6D). Smoothing should be applied carefully in order to preserve the AVP. In Figure 6E the velocity profile at midpoint 175 is depicted for comparison.

Figures 7A/B and 7C/D illustrate the effect of missing data and the benefits of least-squares migration for seismic imaging using a single constant ray-parameter, respectively. The least-squares migrated images delineate the geological structures better than the conventionally migrated incomplete data.

**7 Discussion and conclusion.** In this paper we follow Stolt and Weglein [26] and cast wavefield propagator and recently developed angle imaging techniques within the general framework of scattering theory. It is clear, however, that results based on simplified and linearized modelling and migration formulas have to be interpreted with care. We have

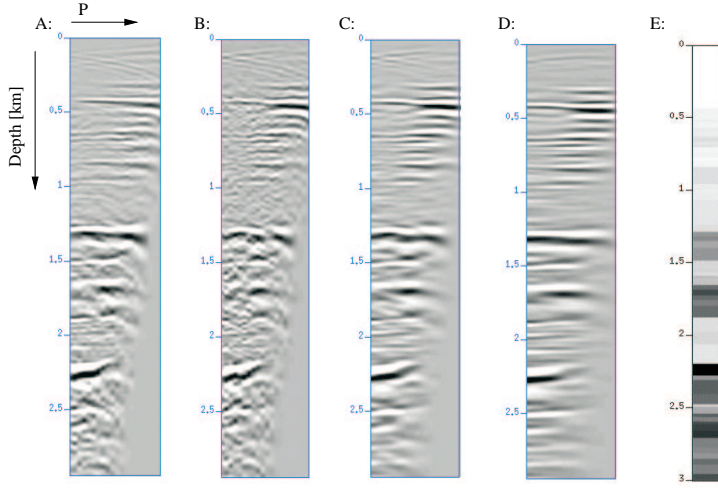


FIGURE 6: AVP gathers and velocity profile of the midpoint location indicated in Figure 5. A: The AVP gather of the complete midpoint dataset obtained by migration. B: The AVP gather of the reduced midpoint data set obtained by migration. About 80% of the data have been randomly removed prior to imaging. C: The same data after 3 iterations of least-squares migration. D: The result after 6 iterations of least-squares migration. E: The velocity profile.

emphasized this point throughout the paper. Nonetheless, AVA/AVP preserved imaging is critical if an interpretation of the properties of the subsurface based on these gathers is to be successful.

The known excellent imaging performance of the propagator methods makes them worthwhile and attractive for migration/inversion in complex media. If care is taken that modelling and migration are adjoint operators we can fit the seismic data by minimizing an appropriate cost function. This approach opens the opportunity to impose certain desirable characteristics and constraints on the least-squares solution. We have exemplified this in a regularization of the least-squares inversion based on ray-parameter dependent smoothing of the AVP gathers. The smoothness constraint helps to mitigate discontinuities that are attributed to incomplete data and numerical operator artifacts and yields an AVP/AVA that exhibits the desired smoothly varying angle dependence.

## LEAST-SQUARES SEISMIC MIGRATION

327

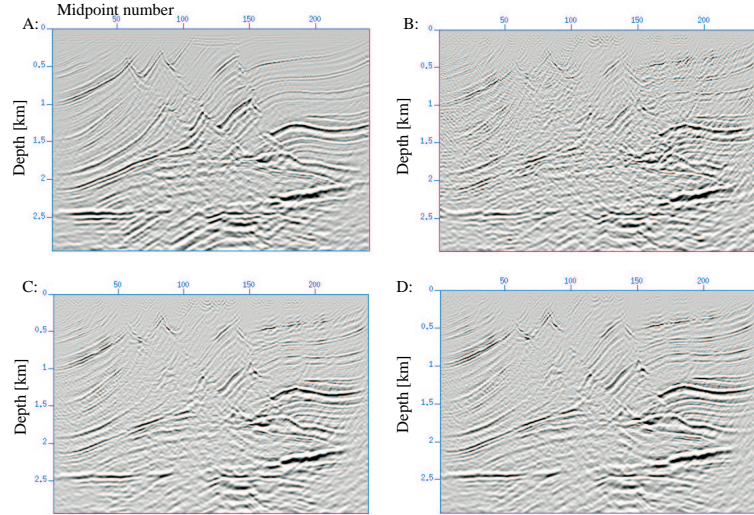


FIGURE 7: Structural images generated with a single constant offset ray-parameter of  $160 \mu\text{s}/\text{m}$ . A: Constant offset ray-parameter migration of the regularly sampled and complete dataset. B: Constant offset ray-parameter migration of the incomplete data (80% of the data were set to zero). C: Least-squares migration with ray-parameter smoothing of the incomplete data after 3 iterations of the conjugate gradients algorithm. D: Result after 6 iterations.

In practice, the incomplete data issue becomes more significant when imaging is to be done in 3 spatial dimensions. This is due to the often encountered sparseness and irregularity of 3-D seismic surveys due to economical and practical reasons. It is conceivable that the least-squares imaging approach becomes particularly beneficial in such cases.

## REFERENCES

1. K. Aki and P. Richards, *Quantitative seismology-theory and methods*. W. H. Freeman and Company, 1979.
2. W. B. Beydon and T. H. Keho, *The paraxial ray method*. Geophysics **52** (1987), 1639–1653.
3. N. Bleistein, *Two-and-one-half dimensional in-plane wave propagation*. Geophysical Prospecting **34** (1986), 686–703.

4. N. Bleistein, J. K. Cohen and J. W. Stockwell, *Mathematics of multidimensional seismic imaging, migration, and inversion*. Springer-Verlag, 2001.
5. J. F. Claerbout, 1992, *Earth Soundings Analysis - Processing versus Inversion*. Blackwell Scientific Publications, 1992.
6. R. W. Clayton and R. H. Stolt, *A Born-WKBJ inversion method for acoustic reflection data*. Geophysics **46** (1981), 1559–1567.
7. C. G. M. de Bruin, C. P. A. Wapenaar and A. J. Berkhouit, *Angle dependent reflectivity by means of prestack migration*. Geophysics **55** (1990), 1223–1234.
8. B. Duquet, J. K. Marfurt and J. A. Dellinger, *Kirchhoff modeling, inversion for reflectivity, and subsurface illumination*. Geophysics **65** (2000), 1195–1209.
9. J. Gazdag, *Wave equation migration with the phase shift method*. Geophysics **43** (1978), 1342–1351.
10. J. Gazdag and P. Sguazzero, *Migration of seismic data by phase shift plus interpolation*. Geophysics **49** (1984), 124–131.
11. S. H. Gray and W. P. May, *Kirchhoff migration using eikonal equation traveltimes*. Geophysics **59** (1994), 810–817.
12. M. R. Hestenes and E. Stiefel, *Methods of conjugate gradients for solving linear systems*. J. Research Nat. Bur. Standards **49** (1952), 409–436.
13. W. Kessinger, 1992, *Extended split-step Fourier migration*. In: 62nd Ann. Internat. Mtg., Soc. Expl. Geophys., Expanded Abstracts, 917–920.
14. H. Kuehl and M. D. Sacchi, *Split-step WKBJ migration/inversion of incomplete data*. 5th SEGJ International Symposium—Imaging Technology, 2001.
15. ———, *Separable offset least-squares DSR migration of incomplete data*. CSEG National Convention, 2001.
16. ———, *Generalized least-squares DSR migration using a common angle imaging condition*. In: 71th Ann. Internat. Mtg., Soc. Expl. Geophys., Expanded Abstracts, MIG 5.6, 2001.
17. ———, *Constrained least-squares wave-equation migration for AVP inversion*. 64th EAGE annual conference, Florence, 2002.
18. G. F. Margrave and R. J. Ferguson, 1999, *Wavefield extrapolation by nonstationary phase shift*. Geophysics **64** (1999), 1067–1078.
19. C. C. Mosher and D. J. Foster, *Common angle imaging conditions for pre-stack depth migration*. In: 70th Ann. Internat. Mtg., Soc. Expl. Geophys., Expanded Abstracts, MIG 4.4, 2000.
20. T. Nemeth, C. Wu and G. T. Schuster, *Least-squares migration of incomplete reflection data*. Geophysics **64** (1999), 208–221.
21. R. Ottolini and J. F. Claerbout, *The migration of common midpoint slant stacks*. Geophysics **49** (1984), 237–249.
22. A. M. Popovici, *Prestack migration by split-step DSR*. Geophysics **61** (1996), 1412–1416.
23. M. Prucha, B. Biondi and W. Symes, *Angle-domain common image gathers by wave-equation migration*. In: 69th Ann. Internat. Mtg., Soc. Expl. Geophys., Expanded Abstracts, 1999, 824–827.
24. P. Sava, B. Biondi and S. Fomel, *Amplitude preserved common image gathers by wave-equation migration*. In: 71th Ann. Internat. Mtg., Soc. Expl. Geophys., Expanded Abstracts, AVO 5.3, 2001.
25. P. L. Stoffa, J. T. Fokkema, R. M. de Luna Freire and W. P. Kessinger, *Split-step Fourier migration*. Geophysics **55** (1990), 410–421.
26. R. H. Stolt and A. B. Weglein, *Migration and inversion of seismic data*. Geophysics **50** (1985), 2458–2472.
27. R. H. Stolt and A. K. Benson, *Seismic Migration: Theory and Practice*. Geological Press, 1986.
28. R. Versteeg and G. Grau (eds.), *The Marmousi experience: Proceedings of the 1990 EAGE Workshop*. 52nd EAGE Meeting, Eur., Assoc. Expl. Geophys., 1991.

## LEAST-SQUARES SEISMIC MIGRATION

329

29. C. P. A. Wapenaar, *Inversion versus migration: A new perspective to an old discussion*. Geophysics **61** (1996), 804–814.
30. ———, *Reciprocity properties of one-way propagators*. Geophysics **63** (1998), 1795–1798.

DEPARTMENT OF PHYSICS, UNIVERSITY OF ALBERTA, EDMONTON, AB, T6G 2J1